Physica B 496 (2016) 74–81

Contents lists available at ScienceDirect

Physica B

journal homepage: www.elsevier.com/locate/physb

X-ray derived experimental charge density distribution in GaF_3 and VF_3 solid systems

K. Sujatha, S. Israel*, C. Anzline, R. Niranjana Devi, R.A.J.R. Sheeba

Research and Post graduate department of Physics, The American college, Madurai 625 002, India

A R T I C L E I N F O

Article history:
Received 22 September 2015
Accepted 29 May 2016
Available online 30 May 2016

Keywords:
Charge density
Multipole analysis
Maximum entropy method
Atomic basins

A B S T R A C T

The electronic structure and bonding features of metal and transition metal fluorides in low oxidation states, GaF_3 and VF_3, have been studied from precise single crystal X-ray diffraction data using multipole and maximum entropy methods. The topology of the charge density is analyzed and the $(3, -1)$ bond critical points are determined. Existences of ionic nature of bonding in low valent fluorine compounds are clearly evident. The spherical core of metal atom and aspherical or twisted core of transition metal atom reveal the fact that GaF_3 is much more rigid than VF_3. Aspherical cores of the polarized ligand atoms are also visible in the two-dimensional density distribution pictures. The true valence charge density surfaces with encapsulating the atomic basins maps are elucidated. An elongated saddle with mid-bond density of 0.6191 e/$Å^3$, observed in the compound VF_3, shows that its lattice is less rigid and has more ionic character than GaF_3.

1. Introduction

Crystallographers do believe that to provide access to the wealth of information about a compound the rationalization of the material properties and the resulting bonding motifs is extremely important. Accurate information about the electronic structure in a crystal is the prerequisite for the evaluation of properties and chemical bonds [1]. In fact, an authoritative and accurate prediction of the electronic structure of the material is possible only by means of charge density research which has the ability to contribute the best solution for the structural problems, rather than any other research. Moreover the technological advances in recent years have offered several user friendly softwares that can yield an accurate charge density analysis.

A great deal of attention has been focused on fluorides due to their peculiar properties and widely used applications in industry as electrochemical devices such as batteries, fuel cells and sensors and channel waveguide in optical communication as it eliminates the transmission loss [2–7]. Fluorides are hard ligands and the least polarisable anion compared to other halides [8]. Indeed, the high electronegative character of fluorine atom invites its applications [9]. These ligands are highly reactive and they form strong bonds with other metals due to the small size of the atom and extremely high oxidizing power [10]. Concept of oxidation states is one of the most important classifications within the general and fundamental bonding principles in fluorides. Fluorides of metals and transition metals in low valence states are mostly ionic, but in high valence states they tend to be polar covalent [11]. This has been confirmed by Israel et al. [12] and Saravanan et al. [13] in their study of bonding features of some fluorine compounds in low oxidation states. The crystal structure and bonding features of metal fluorides are mainly governed by Pauling's rules [14], geometric and electrostatic principles. But in case of transition metal ions, the crystal structures and bonding of compounds are affected by a variety of electronic effects such as spin state, back-bonding, Jahn-Teller distortion and ligand field splitting [15]. In addition to this, according to Ian Bytheway [16], the cores of the atoms which have an incomplete d-sub shell as in the case of transition metals and those of the polarized ligands may not be spherical. Hence the basic motivation of this work is to undertake a study on bonding in low valent metal and transition metal fluorides and to interpret the deviations from geometric and electrostatic principles, which governs the crystal structures, caused by bonding and electronic effects.

As proposed by Hepworth et al. [17], most of the metallic triflourides fall into three types of structures :(i) cubic closely packed structure, e.g. MoF_3 and TaF_3 [18] ; (ii) hexagonal closely packed structure, such as RhF_3, PdF_3 and IrF_3; (iii) intermediate between the cubic structure and hexagonal structure, typified by RuF_3. The low valent metal triflouride, GaF_3 falls into the third category which has a rhombohedral structure with $R\bar{3}c$ space group symmetry. Each gallium atom is surrounded by six fluorine atoms and each fluorine atom is surrounded by two gallium atoms. This structure of gallium triflouride has been confirmed by Brewer et al.

---

* Corresponding author.
E-mail address: israel.samuel@gmail.com (S. Israel).

http://dx.doi.org/10.1016/j.physb.2016.05.032
0921-4526/© 2016 Elsevier B.V. All rights reserved.

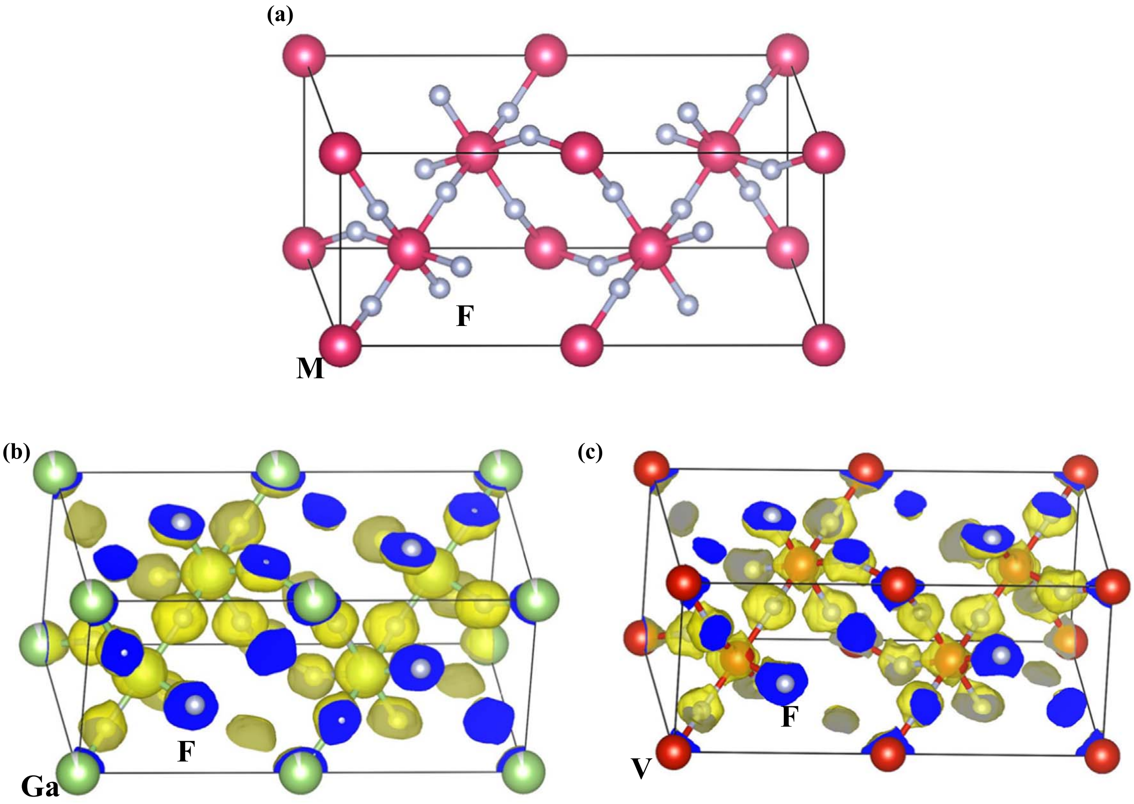

Fig. 1. (a). Isostructural unit cell of MF_3 (M=Ga, V). 3- dimensional charge density distribution in (b) GaF_3 and (c) VF_3 unit cell. The isosurface level is 0.85e/Å^3.

Table 1
Results of least squares refinement.

Parameters	GaF_3	VF_3
a (Å)	4.9681	5.1766
b (Å)	4.9681	5.1766
c (Å)	12.9663	13.3063
Cell Volume(Å^3)	277.1575	300.003
Density (gm/cc)	4.3994	3.4813
B_{iso}(Å^2)	Ga - 0.3414	V - 0.4094
B_F(Å^2)	0.3654	0.4906
R_{obs} (%)	0.94	1.34
wR_{obs} (%)	1.23	2.10

[19] and recently the parameters have been refined by Roos et al. [20].

Glemser [21] categorized the structures of transition metal fluorides in to three types as same as Hepworth categorized the metal triflourides. Based on this, the transition metal trifluoride, VF_3 crystallizes in the GaF_3 type of structure with a rhombohedral structure and $R\bar{3}c$ space group symmetry. The isostructural unit cell of MF_3 (M=Ga,V) is shown in Fig. 1(a). The first work on this fluoride was carried out by Jack et al. [22] and the crystal structure has been elucidated. Similar to the gallium atoms in GaF_3, each vanadium atom is surrounded by six fluorine atoms and each fluorine atom is surrounded by two vanadium atoms. The vibrational studies of VF_3 were carried out by Daniel et al. [23] and Bukhmarina et al. [24]. Basically, the transition metals form compounds which have paramagnetic or diamagnetic behavior. The V^{3+} ion exhibits paramagnetic nature, as suggested by Telser et al. [25]. More recently the structure of VF_3 was reported by Ali Rahmani et al. [26] theoretically. Though the crystal structure of GaF_3 and VF_3 have been reported by few researchers, the clear evidence of the bonding between the metal/ transition metal atoms and fluorine atoms has not been investigated. Hence in the present work a precise study on bonding in both the crystals has been undertaken by using multipole and MEM analysis of experimentally derived charge density using X-ray diffraction data.

2. Preparation

A mixture of gallium metal (Ventron 4 N) and NH_4F (Merck 99.8%), which is recrystallized from CH_3OH to remove the traces of water, in a molar ratio of 1:3, is taken in a sealed Monal container. A temperature of 748 K is maintained for crystallization for a period of 6 weeks. GaF_3, as thus prepared, is colourless, square shaped crystals.

A similar procedure proposed by Jerome [27] was adopted for the growth of VF_3 crystal. 1.6 g of VF_3 powder in 1.5 cc of 49% HF was taken in a sealed platinum tube. The reaction temperature of 450 °C with a crystallization time of 60 h yielded yellow green nearly cubic VF_3 crystals after cooling by hydrothermal synthesis.

Using Nonius crystal spherizer, small spheres of GaF_3 and VF_3 were prepared from bulk crystals. Good quality crystals were chosen and the strained surfaces were removed using suitable etching solutions. The X-ray intensity data collection was carried out with a Bruker Smart Apex CCD area detector using a graphite monochromated MoKα radiation (λ=0.71073 Å) at room temperature. Thus full data sets were collected for GaF_3 and VF_3 for present study.

3. Methodology

3.1. Least squares refinement

The raw structure factors for both the GaF_3 and VF_3 data sets were refined using anharmonic model, with prior corrections for

Table 2
Isotropic and anisotropic parameters.

Atoms	Reference	B_{iso}(Å^2)	U_{11}	U_{22}	U_{33}	U_{12}	U_{13}	U_{23}
Ga	Present work	0.3414	0.0027	U_{11}	0.0048	0.0013	0	0
	[17]	0.05792	0.0033	U_{11}	0.0030	0.0016	0	0
F	Present work	0.3654	0.0309	U_{11}	0.0276	0.0146	−0.0027	0.0027
	[17]	0.0208	0.0090	U_{11}	0.0083	0.0057	−0.0020	0.0027
V	Present work	0.4094	0.0034	0.0034	0.0046	0.0017	0	0
	[20]	0.42	0.0051	0.0051	0.006	0.0026	0	0
F	Present work	0.4906	0.0057	0.0014	0.0101	0.0007	−0.0044	−0.0088
	[20]	0.96	0.0122	0.0106	0.0132	−0.0053	−0.0027	−0.0054

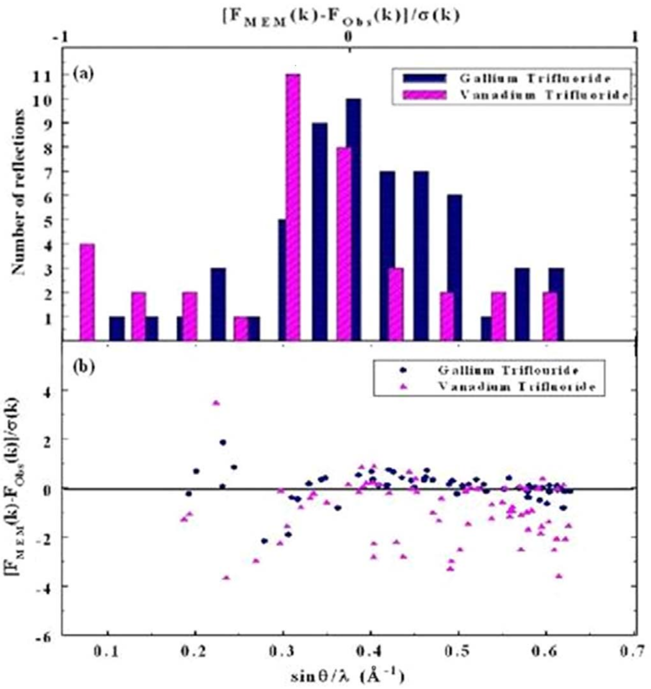

Fig. 2. (a). Histogram of observed number of reflections. (b). Error distribution of the observations in reciprocal space.

Table 3
Results of multipole refinement.

Parameters	GaF$_3$		VF$_3$	
	Ga	F	V	F
P_C	18.0645	1.93	18.0331	2.0043
P_V	11.9575	6.9868	5.1961	7.2700
κ	1.0029	1.0006	0.7887	0.9462
κ'	1.2625	0.8364	1.0000	1.0000

absorption [28] and extinction effects using a Zachariasen model [29] and for Thermal Diffuse Scattering parameters (TDS) using a standard least squares full matrix method.

In this method,

$$D=\sum_{hkl} W_{hkl}\left(|F_O|-|F_C|\right)^2$$

is the quantity to be minimized and hence, is the principle of this method. Here W_{hkl} is the weight to be assigned to an observation and F_O and F_C are the observed and calculated structure factors.

3.2. Charge density estimation

3.2.1. Multipole model refinement

A versatile refinement technique called the multipole model refinement based on the aspherical electron density model proposed by Hansen and Coppens [30] was used in the present work to understand the contraction/expansion of atoms in the compound. According to this model, the charge density given by the equation,

$$\rho(r)=\sum_{k}^{atoms}\rho(r-r_k-u)\otimes t_k(u),$$

consists of superposition of harmonically vibrating aspherical atomic density distribution. In this equation $t_k(u)$ is the Gaussian thermal displacement and the symbol ⊗ is the convolution. The atomic density described as a series expansion in real harmonic functions through fourth order Y_{lm} is defined by,

$$\rho(r)=P_c\rho_{core}(r)+P_v\kappa^3\rho_{valence}(\kappa r)+\sum_{l=0}^{4}\kappa'^3R_l(\kappa' r)+\sum_{m=-1}^{l}P_{lm}Y_{lm}\left(\frac{\vec r}{r}\right)$$

where P_c, P_v and P_{lm} are population coefficients. For the construction of ρ_{core} and $\rho_{valence}$, canonical Hartree – Fock orbitals of free electrons normalized to one electron can be used, but the expansion or contraction of valence function was achieved by adjusting the variable parameters κ and κ'. The dynamic and static multipole deformation maps indicate the convoluted and deconvoluted form of thermal contribution. The difference in densities in these maps are characterized by,

$$\Delta\rho_{multipole-deformation}(\vec r)=\frac{1}{V}\sum\left[F(\vec h)_{multipole}-F(\vec h)_{spherical-atom}\right]\exp\left[-2\pi i(\vec h-\vec r)\right]$$

where $F_{multipole}$ is the Fourier transform of the multipole charge density with or without the convolution of thermal contribution and the fourier components are terminated at the experiment resolution. The multipole model refinement is done by using the software JANA 2006 [31] for core, valence and pseudo-atomic electron occupancies.

The charge density distribution constructed by using multipole model is analyzed in detail by the topological view of the electron density using, “Atoms In Molecules (AIM) theory”, as proposed by Bader [32]. According to him, “two atoms are bonded if they are connected by a line of maximum electron density called a bond path, on which lies a bond critical point (BCP) where $\vec\nabla\rho(r_{BCP})=0$, and the critical points are the characteristics of the bond existing between the atoms”.

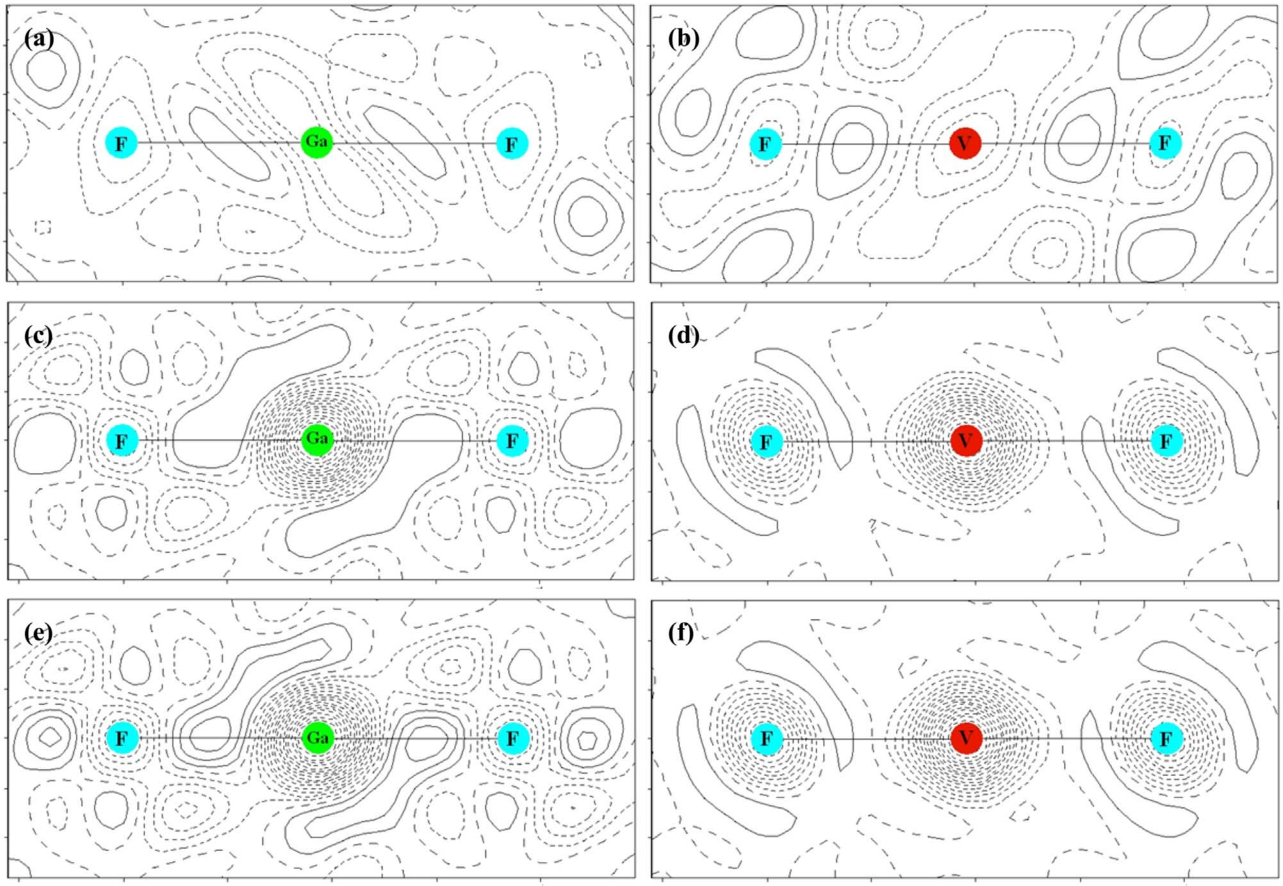

Fig. 3. Difference Fourier maps of (a) GaF_3 and (b) VF_3, Dynamic deformation multipole density maps of (c) GaF_3 and (d) VF_3 and Static deformation multipole density maps of (e) GaF_3 and (f) VF_3 . Negative contours are shown with dashed lines.

Table 4
(3, − 1) Bond critical points.

Bond	Critical point	d	d_1	d_2	ρ
Ga–F	(3, − 1)	1.8994	0.9086	0.9908	0.7190
V–F	(3, − 1)	1.9829	0.8725	1.1104	0.6191

Table 5
Results of the MEM refinement.

Parameters	GaF_3	VF_3
Lagrange parameter	0.011029	0.009867
Number of cycles	726	1593
Prior electron density (e/Å^3)	1.2159	0.9715
Resolution (e/Å^3/pixel)	0.08	0.08
R_{obs} (%)	0.70	1.67
wR_{obs} (%)	1.0004	2.0706

3.2.2. Mem refinement

The best mathematical tool for the clear visualization of chemical bonds and for obtaining the density distribution of charges is the maximum entropy method (MEM), a statistical as well as probabilistic approach proposed by Collins [33]. The structure factors from the refinement were used for MEM refinements. According to Collins, the electron density at the ith pixel is

$$\rho(r_i) = \tau(r_i)\exp\left[\left(\frac{\lambda F_{000}}{N}\right)\sum\left[1/\sigma(k)\right]^2\left|F_{Obs}(k) - F_{Cal}(k)\right|\exp(-2\pi jk.\ r)\right]$$

where $\tau(r_i)$ is the prior electron density and F_{000} is the number of atoms in the unit cell. When $\sigma(k)$, $F_{Obs}(k)$ and the Lagrange's multiplier λ are given, $\rho(r_i)$ could be obtained which is the desired MEM estimate for $\rho_{mem}(r_i)$, the electron density distribution.

The software PRIMA [34,35], which employs the maximum entropy method is used for the evaluation of charge density and the visualization software VESTA [36] is used to plot the resultant density.

4. Results and discussion

The raw intensity data of GaF_3 and VF_3 were refined by using least-squares refinement method. Exact matching of the observed and calculated structure factors were realized. The results of the full matrix least-squares refinements are given in Table 1. The reliability index (R) values, given by the equation $R=\sum\left|\left|F_{Obs}\right| - \left|F_{Cal}\right|\right|/\sum\left|F_{Obs}\right|$, are very low (0.94 for GaF_3 and 1.34 for VF_3) and this indicates the correctness of the models adopted for both refinements and also that the data is suitable for charge density studies.

From the Debye-Waller factors presented in the Table 1 it is clear that in both the systems GaF_3 and VF_3 the fluorine atom has large thermal vibration compared to the constituent atoms Ga and V. Here, the universal fact that the lighter F atom (Z(F)=9) vibrating more than the heavier atoms (Ga and V) is realized. In addition to this, the thermal parameter of fluorine atom is larger in VF_3 than in GaF_3. The difference in B_F between GaF_3 and VF_3 is 0.1252(Å^2). This indicates that GaF_3 has slightly larger binding force than VF_3 which is due to the more number of electrons

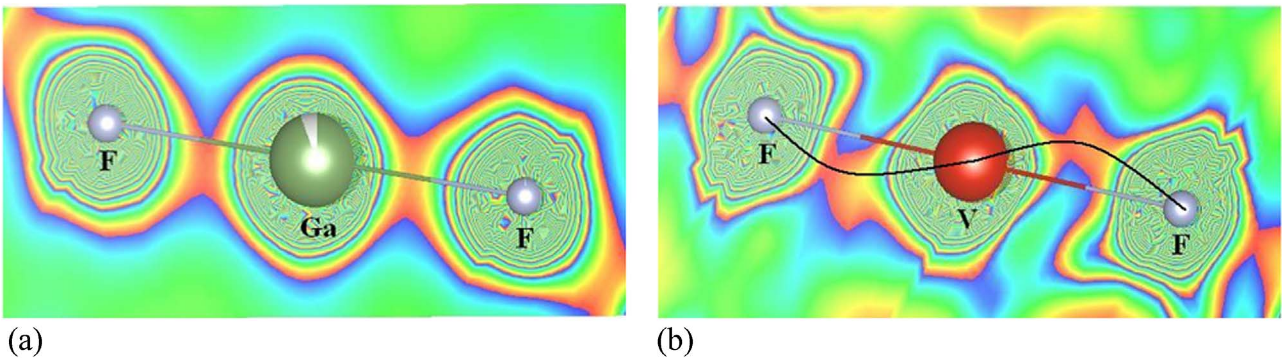

Fig. 4. Two-dimensional MEM electron density map of (a) GaF_3 and (b) VF_3.

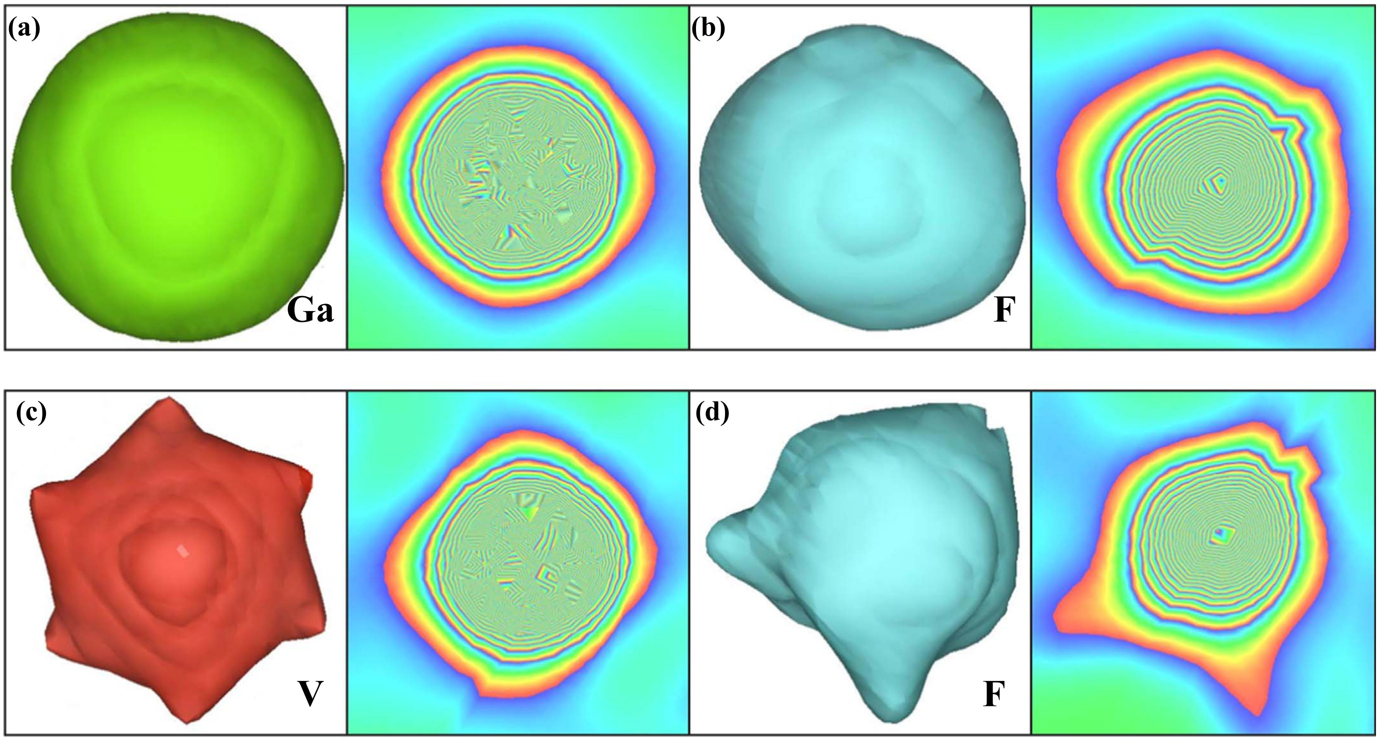

Fig. 5. Shapes of atomic basins and cross-sections of (a) Ga, (b) F in GaF_3, (c) V and (d) F in VF_3.

present in the former than the latter. The isotropic and anisotropic parameters for Ga, V and F atoms are compared with the reported values in Table 2.

To undertake a charge density study, a good quality data with reflections having negligible or minimum error is required. Hence the data were checked by using two methods. Primarily, a histogram is drawn (Fig. 2(a)) with $[F_{MEM}(k)–F_{Obs}(k)]/\sigma(k)$ versus the number of reflections and the expected Gaussian form is obtained. Secondarily, the error distribution of structure factors in the form of $[F_{MEM}(k)–F_{Obs}(k)]/\sigma(k)$ in the reciprocal space is plotted and is given as Fig. 2(b). The graph shows the spread of errors within a minimum value of ± 4 and this indicates the precision of the unbiased errors in the observations throughout the reciprocal lattice space. Thus after confirming the quality of the data being good, the charge density study was proceeded.

One of the more reliable model for charge density estimation is multipole formalism. Hence the multipole analysis is done for the core, valence and pseudo-atomic electron occupancies P_{lm} by using the software JANA 2006 [31]. From Clementi tables [37], the neutral atom wave functions are taken and the Slater type radial functions with $n_l = 4\,4\,6\,8$ and $n_l = 2\,2\,2\,3$ for Ga/V and F respectively for $l \leq 4$ are used according to Hansen and Coppens. The core charges were taken as Ar for Ga/V and He for F atom during refinement. The valence expansion/contraction parameter (κ) is refined for individual atoms in both GaF_3 and VF_3 data sets. The results of the refinement are presented as Table 3. The refined values of κ and κ' show expansion when they assume value less than 1 and contraction when they being greater than 1. The values of κ for Ga,V and F atoms in the table show some interesting results. The κ for F atom is found to be 1.0006 in GaF_3 and 0.9462 in VF_3. These values show that F atom has undergone contraction in GaF_3 and expansion in VF_3 while bonding. Both the Ga and F atoms contract in GaF_3 from their original size and both the V and F atoms expand in VF_3 while bonding. The sum of the core and valence charges (P_c and P_v) of Ga and F atoms in GaF_3 are 30.022 and 8.9168 respectively. These values are less than the actual Z values. Hence it confirms the contraction of both the atoms in the molecule. Similarly, the sum of P_c and P_v values of V and F atoms in

VF_3 are 23.2292 and 9.2743 respectively and thus it confirms the expansion of both the atoms, since these values are greater than the actual Z values of the atoms. In both the cases the charges are either spilled out or included into the atomic basins. The κ' of VF_3 could not be refined, as it is found that V undergoes a high aspheric deformation when it binds with F. This results in the unpredictable zero flux surface in all crystallographic directions which makes the κ' difficult to refine. This is also a primary reason why the charge integration in V and F gave some unphysical or excess values than the atomic number.

The refined structure factors were used for the construction of multipole maps. The difference fourier maps, thus constructed for GaF_3 and VF_3 shown in Fig. 3(a) and (b) respectively, indicates less noise and background density and thus it confirms the better quality of the data. The dynamic and static deformation maps are constructed to see the effect of temperature on the charge distribution and are given as Fig. 3(c) and (e) for GaF_3 and Fig. 3(d) and (f) for VF_3. Both the maps indicate less deformation of Ga/V and F atoms.

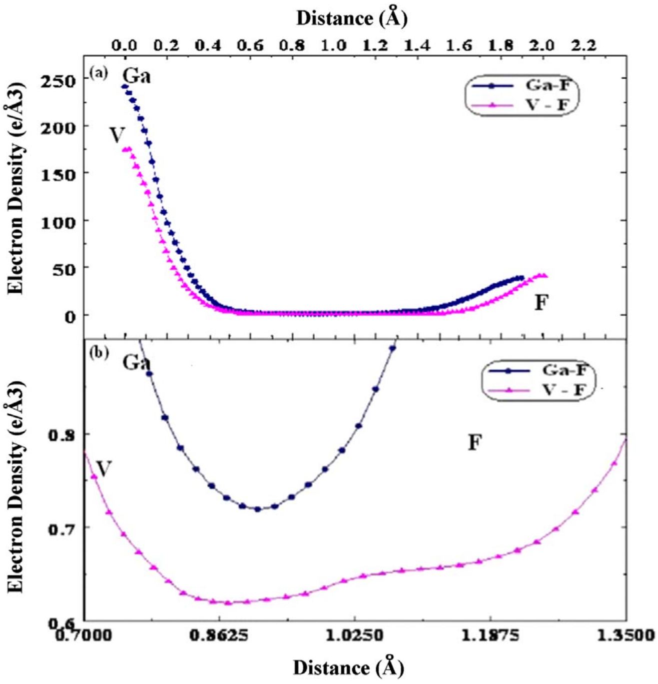

Fig. 6. (a). One-dimensional electron density distribution. (b). Valence charge density distribution.

Using the Newton-Raphson method, the $(3,-1)$ bond critical points (BCP) are searched in the charge density distribution of GaF_3 and VF_3 and presented as Table 4. The $(3,-1)$ CPs characterize the bonding. In the table, d, d_1 and d_2 represents the distance between Ga/V and F, Ga/V and CP and CP and F respectively and ρ is the density at the bond critical point. The absence of the Non Nuclear Maxima (NNM) at the BCP is an evidence for the ionic nature of bonding between Ga/V and F atoms in both the materials. The ionic and covalent radii of Ga are 0.62 and 1.26 and that of V are 0.74 and 1.22 respectively. The value of d_1 in GaF_3 (0.9086 Å) lies between those of r_i and r_c of Ga. This shows a mixed ionic and covalent character in the molecule. Even though, the absence of NNM confirms that the ionic nature predominates in GaF_3. But in case of VF_3, as the d_1 value approaches the r_i value of V, the bonding in VF_3 is highly ionic with slight covalent nature. Moreover, the charge density at the bond critical point is larger in GaF_3 than in VF_3. This confirms the high ionic character in VF_3 than in GaF_3.

Another more reliable and sophisticated model for charge density estimation is Maximum Entropy Method (MEM). A more clear visualization of the bonding features can be attained by this method. The structure factors from the least-squares refinement were used for the MEM refinements. Initially the unit cell of GaF_3 as well as VF_3 is divided so as to contain $64 \times 64 \times 164$ pixels. The prior charge density assigned to each pixel is F_{000}/a^3(1.2159 for GaF_3 and 0.9715 for VF_3). The convergence criterion, $C=1$ was achieved after 726 and 1593 iterative cycles for GaF_3 and VF_3 respectively. The parameters of the refinements are given in Table 5. The reliability index values are very low ($R_{MEM}=0.7\%$ for GaF_3 and 1.67% for VF_3) and this, again implies the better quality of the data. The resolution of the maps turns out to be 0.08 $Å^3$ for both the materials along the three directions of the unit cell. The 3-dimensional charge density maps obtained, which are presented as Fig. 1(a) and (b) for GaF_3 and VF_3 respectively, show the shape of the constituent atoms and their valence charge density in real space.

Fig. 4(a) and (b) represents the two-dimensional electron densities of GaF_3 and VF_3 respectively along the bonding direction. In Fig. 4(a), as it shows the bonding between the metal and ligand atoms, the metal atom (Ga) at the centre is perfectly spherical and thus it indicates that the bond is packed. Because of this perfect bonding, the gallium atom has less space to vibrate which reflects

Table 6
Bond lengths and bond angles.

Bond lengths and bond angles	GaF_3				VF_3				
	Present work		[16]	[17]	Present work		[19]	[20]	[22]
	MEM	Multpole			MEM	Multipole			
M–F (Å)	1.869(3)	1.870(2)	1.89	–	1.918(2)	1.918 (5)	1.95	1.935(1)	2.5946
								1.94 (6)	2.6137 2.2902
M–M(Å)	3.591(3)	3.591(1)	3.61	–	3.7217(1)	3.722(3)	3.73	–	–
F–F(Å)	2.6449(3)	2.643 (3)	2.69	–	2.7106(2)	2.7106(1)	2.74	2.734(4)	–
	2.641(3)	2.646 (2)	2.67		2.714 (3)	2.714(2)	2.75	2.74(4)	
	2.645(3)	2.646 (2)			2.711(1)	2.711(1)		2.75(4)	
(F–M–F)°	89.92(2)	89.93(1)	–	–	89.92(2)	89.92(2)	–	89.89(3)	86.14
(M–F–M)°	147.82(1)	147.88(2)	145	147.79(8)	151.9(3)	151.95(2)	–	149.06(9)	142.33

the low B_{iso} value in Table 2. The slight deviation in spherical shape of the fluorine atom is due to its polarizing nature. But in case of Fig. 4(b), which shows the bonding between the transition metal and ligand atom, the cores of both the transition metal atom (V) and polarized ligand atom (F) are not spherical as viewed by Ian Bytheway [16] in his study of the structures of transition metal fluorides [16]. The asphericity of the core of the vanadium atom may be due to its paramagnetic character also as suggested by Telser et al. [25]. Due to this twisting of atoms, the bond is also twisted. Thus the vanadium atom has many degrees of freedom and more space to vibrate. This reflects the large B_{iso} value of V atom in Table 2. Because of the twisting of V atom, F atom is also distorted and this enables the availability of large space for the vibration of F. This reflects the larger B_{iso} value of F in VF_3 than in GaF_3. Since the bond path itself is bent, the BCP is not lying at the bond axis and it lies at the off-axis. This twisting of V atom and the position of CP at the off-axis interprets the low value of ρ of VF_3 in Table 4. Hence the attempt to measure the bond length (V–F) in VF_3 actually offered the length of the bond path, and not the bond length. Thus, from the bonding nature of the two compounds it is clearly evident that metal fluoride (GaF_3) is much more rigid than transition metal fluoride (VF_3) and the transition metal fluoride (VF_3) is fragile. For the clear visualization of the spherical and aspherical nature of atoms, the true valence charge density surfaces were drawn by identifying zero flux surface (ZFS) at all directions which encapsulates the atomic basins and their cross-sections and are presented as Fig. 5(a), (b), (c) and (d). Atoms which have high electronegative character, should obviously occupy larger atomic basin volume. Confirming this fact, F atoms having high electronegative character of about 3.98, was found to occupy larger atomic basin volume than the other two atoms (Ga and V). Comparing Ga and V, the electronegativity of Ga ($\chi = 1.81$) is slightly larger than V ($\chi = 1.63$) and hence the atomic basin of Ga is larger than V. All these informations are clearly visualized from the drawn atomic basins presented in Fig. 5.

While discussing about the type of bonding existing between the atoms in both the compounds, in both the Fig. 4(a) and (b), it is clear that Ga/V and F atoms are well resolved and there is no Non Nuclear Maxima (NNM) found at the mid-bond region. Thus a clear ionic nature of bonding is seen in GaF_3 and VF_3.

To visualize a precise bonding density distribution and to quantify the strengths of bonding, one-dimensional electron distribution profile was drawn and given as Fig. 6(a). From the figure, it is noted that there is no indication of NNM in the profile. Thus the bonding between Ga/V and F atoms is predominantly ionic. In GaF_3, at the saddle point (0.9086 Å) the electron density is 0.7190e/Å^3 and in VF_3, it is 0.6191e/Å^3 at 0.8725 Å. The low value of mid-bond density of VF_3 than that of GaF_3 confirms that the former exhibits more ionic nature than latter. The valence charge density distribution in one-dimension was drawn and presented as Fig. 6(b). This shows the clear picture of the bent bond path of VF_3 in one-dimension. Thus its profile has an elongated saddle and hence the valence charges are extended in the compound. The bond lengths and bond angles of GaF_3 and VF_3 are compared with the reported ones in Table 6.

Analysing the charge density estimation by both multipole and maximum entropy methods, it is concluded that GaF_3 has larger mid-bond density and shorter bond length than VF_3. And also the bond path in GaF_3 is a straight line, while in VF_3 it is twisted as its core is twisted. This indicates that GaF_3 is a hard molecule than VF_3. The values of the Debye-Waller factors also confirm that, as a molecule, GaF_3 is tightly bound and VF_3 is loosely bound. In case of bonding nature, VF_3 is more ionic than GaF_3.

5. Conclusion

A precise charge density analysis has been carried out in metal fluoride GaF_3 and transition metal fluoride VF_3 using single crystal X-ray data. The expansion and contraction of individual atoms are analyzed by multipole methods. The existence of ionic nature of bonding in fluoride compounds in low valence states is clearly revealed qualitatively as well as quantitatively using maximum entropy methods. The deviations in spherical nature of cores of the transition metal and ligand atoms are also interpreted. Similar studies on other fluoride compounds would enhance the knowledge about their bonding and electronic structures which in turn increases the utility of the materials.

References

[1] R. Saravanan, M.Prema Rani, Metal and Alloy Bonding: An Experimental Analysis, Springer-Verlag London Limited, 2012.
[2] Dayaldas T. Meshri, Industrial Applications of Inorganic Flourides, Elsevier Science S.A., 2000.
[3] Neil Bartlett, Introductory Remarks, Elsevier Science S.A, 2000.
[4] Jean-Luc Adam, Optical Properties and Applications of Flouride Glasses, Elsevier Science S.A., 2000.
[5] Kiyoshi Kanamura, Flourine compounds in Battery Applications, Elsevier Science S.A., 2000.
[6] John Emsley, Nature's Building Blocks: An A-Z Guide to the Elements, 2nd Edition, Oxford University Press, New York, 2011.
[7] Glenn G. Amatucci, Nathalie Pereira, Flouride based electrode materials for advanced energy storage devices, J. Flourine Chem. 128 (2007) 243–262.
[8] John H. Holloway, Eric G. Hope, Novel synthesis using inorganic fluorides, J. Flourine Chem. 76 (1996) 209–212.
[9] A. Trueba, P. Garcia-Fernandez, J.M. Garcia-Lastra, J.A. Aramburu, M.T. Barriuso, M. Moreno, Transition metal impurities in fluorides: role of electronic structure of fluorine on spectroscopic properties, J. Flourine Chem. 132 (2011) 747–754.
[10] Karel Lutar, Horst Borrmann, Marc Leblanc, Recent Developments in the Synthesis of Inorganic Flourides, Elsevier Science S.A., 2000.
[11] Andrew R. Barron, "Compounds of Flourine", OpenStax-CNX module: m33815, 2010, pp. 1–4.
[12] S. Israel, R. Saravanan, N. Srinivasan, R.K. Rajaram, High resolution electron density mapping for LiF and NaF by maximum entropy method (MEM), J. Phys. Chem. Solids 64 (2003) 43–49.
[13] R. Saravanan, S. Israel, Bonding in fluorite compound CaF_2 using MEM, Phys. B 352 (2004) 220–226.
[14] Linus Pauling, Pauling rules for ionic structures, J. Am. Chem. Soc. 51 (4) (1929) 1010–1026.
[15] Werner Massa, Dietrich Babel, Crystal structure and bonding in transition metal fluoro compounds, Chem. Rev. 88 (1) (1988) 275–296.
[16] Ian Bytheway, Ronald J. Gillespie, Structures of some transition metal fluorides and oxoflourides and the VSEPR model, J. Flourine Chem. 71 (1995) 189.
[17] M.A. Hepworth, K.H. Jack, R.D. Peacock, G.J. Westland, The crystal structures of the triflourides of Iron, Cobalt, Ruthenium, Rhodium, Palladium and Iridium, Acta. Cryst. 10 (1957) 63–69.
[18] V. Gutmann, K.H. Jack, The crystal structures of Molybdenum Triflouride, MoF_3 and Tantalum Triflouride, TaF_3, Acta Cryst. 4 (1951) 244.
[19] F.M. Brewer, G. Garton, D.M.L. Goodgame, The preparation and crystal structure of gallium triflouride, J. Inorg. Nucl. Chem. 9 (1959) 56–64.
[20] M. Roos, G. Meyer, Refinement of the crystal structure of gallium triflouride, GaF_3, Z. Kristallogr. NCS 216 (2001) 18.
[21] O. Glemser, The structure of some transition metal fluorides, J. Flourine Chem. 24 (1984) 319–325.
[22] K.H. Jack, V. Gutmann, The crystal structure of vanadium triflouride VF_3, Acta Cryst. 4 (1951) 246–249.
[23] P. Daniel, A. Bulou, M. Leblanc, M. Rousseau, J. Nouet, Structural and vibrational study of VF_3, Mat. Res. Bull. 25 (1990) 413–420.
[24] V.N. Bukhmarina, A.Yu Gerasimov, Yu.B. Predtechenskii, Vibrational spectra of matrix isolated VF_3 and CoF_3, Vibrational Spectroscopy 4 (1992) 91–94.
[25] J. Telser, C.C. Wu, K.Y. Chen, H.F. Hsu, D. Smirnov, A. Ozarowski, J. Krzystek, Aminocarboxylate complexes of vanadium (III): electronic structure investigation by high-frequency and -field electron paramagnetic resonance spectroscopy, J. Inorg. Biochem. 103 (4) (2009) 487–495.
[26] Ali Rahmani, Structural properties of theoretical studies of Vanadium (III) fluoride and Molybdenum (III) fluoride Compounds, Flourine notes 4 (89) (2013).
[27] Jerome Lhoste, Karim Adil, Armel Le Bail, Marc Leblanc, Annie Hemon-Ribaud, Vincent Maisonneuve, Mixed metal^{II}-metal^{IV} hybrid fluorides, J. Flourine Chem. 134 (2010) 29–34.
[28] International Tables for X-ray Crystallography, Vol. IV, The Kynoch Press, England, 1974.
[29] W.H. Zachariasen, Acta Cryst. 23 (1967) 558.
[30] N.K. Hansen, P. Coppens, Acta Cryst. A34 (1978) 909–921.
[31] V. Petříček, M. Dušek, L. Palatinus, JANA, The Crystallographic Computing System, Institute of Physics Academy of sciences of the Czech republic, Praha, 2006.

[32] R.F.W. Bader, Atoms in molecules—A quantum theory, Oxford Univ. Press, Oxford, 1990.
[33] M. Collins, Nature 298 (1982) 49.
[34] R.A. Dilanian, F. Izumi, Super-fast Program, PRIMA, for the Maximum Entropy Method, 2005.
[35] F. Izumi, R.A. Dilanian, Recent Research Developments in Physics, Vol. 3, Part II, Transworld Research Network, Trivandrum, 2002, pp. 699.
[36] K. Momma, F. Izumi, VESTA, Visualisation for Electronic and Structual analysis, Commission on Crystallogr. Comput., IUCr Newslett., 2006, No. 7:106.
[37] E. Clementi, C. Roetti, Roothaan-Hatree-Fock atomic wave functions, At. Data Nucl. Data Tables 14 (1974) 177–478.